Development and application of aberration-compensating x-ray phase-retarder systems

Kouhei Okitsu[a],Yoshinori Ueji[b] and Yoshiyuki Amemiya[b]

[a]Institute of Engineering Innovation, School of Engineering, The University of Tokyo, 2-11-16 Yayoi, Bunkyo-ku, Tokyo 113-8656, Japan

[b]Department of Advanced Materials Science, Graduate School of Frontier Sciences, The University of Tokyo, 5-1-5, Kashiwanoha, Kashiwa-shi, Chiba 277-8561, Japan

ABSTRACT

X-ray phase-retarder systems to compensate for aberrations which arise from angular divergence and energy spread of x rays, have been developed. The two-quadrant x-ray phase-retarder system consists of two diamond crystals of almost identical thickness. It can compensate for off-axis aberration (phase-shift inhomogeneity due to angular divergence of incident x rays) The four-quadrant x-ray phase-retarder system consists of four diamond crystals of almost identical thickness. The scattering planes of four phase retarders were set to be inclined by 45 deg, 135 deg(= 45 deg +90 deg), 225 deg(= 45 deg +180 deg) and 315 deg(= 45 deg +270 deg), respectively, with respect to the direction of incident polarization. It can compensate for not only the off-axis aberration but also chromatic aberration (phase-shift inhomogeneity due to energy spread of incident x rays) The principles and applications of the two-quadrant and four-quadrant phase-retarder systems will be described.

Keywords: x-ray diffraction, x-ray phase retarder, x-ray phase plate, diamond, dynamical diffraction theory, x-ray polarization, polarized x rays

1. INTRODUCTION

After the discovery of x-ray diffraction by Laue in 1912, dynamical diffraction theories which describe the behavior of x rays diffracting in a perfect crystal, were constructed from 1910's to 1930's by Darwin, Ewald and Laue. Based on the dynamical diffraction theory, Moliere[1] pointed out that polarization analysis of x rays would be feasible as in the visible light range when diffracting perfect crystals were used as polarization optical devices for x rays. This suggestion was, however, not realized for a long time since crystal-growth technology in those days had almost no chance to obtain a crystal with sufficient perfection. Since crystal-growth methods to obtain silicon crystals with extremely high perfection were developed in late 1950's, this technology stimulated again theoretical and practical studies on the x-ray dynamical diffraction theory. With this background, Skalicky and Malgrange[2] suggested a feasibility of x-ray phase retarder utilizing a perfect crystal. From that time on, in cooperation with synchrotron radiation, several candidates of reflection-type phase retarder utilizing x rays Bragg-reflected by perfect crystals were suggested by several authors[3–7] but didn't reach general practical use. In this period, Hart and Rodrigues[8] developed energy-tunable x-ray polarizer and analyzer working with extremely high extinction ratio (reflectivity ratio of σ- to π-polarization $> 10^4$).

In 1991, Hirano, Ishikawa, Kikuta and their co-authors[9–15] developed the transmission-type x-ray phase retarder using x rays transmitted by a Bragg-reflecting perfect crystal in the vicinity of the Bragg condition. While both reflection- and transmission-type x-ray phase retarders utilize phase shift between σ- and π-polarized x rays with a Bragg-reflecting perfect crystal, Hirano and his co-workers noticed that dependence of phase shift between σ and π polarizations of transmitted x rays on x-ray incident angle was extremely small compared with that of Bragg-reflected x rays. Early applications of the transmission-type phase retarder to x-ray magnetic circular dichroism (XMCD) were reported by Giles *et al.*,[16] Hirano and Maruyama[17] and Suzuki *et al.*[18]

2. TWO-QUADRANT PHASE-RETARDER SYSTEM

2.1. Principle of compensation for off-axis aberration

In spite of the advantage of the transmission-type phase retarder over the reflection-type phase retarder, collimation of x rays incident on the transmission-type phase retarder is necessary when strictly defined state of polarization is demanded, as pointed out by Hirano, Ishikawa and Kikuta.[13] According to Hirano, Ishikawa and Kikuta,[14] when deviation angle $\Delta\theta$ from the Bragg

Further author information: (Send correspondence to K. O.)

K. O. : E-mail: okitsu@soyak.t.u-tokyo.ac.jp, Telephone: 81 3 5841 7470

Crystals, Multilayers, and Other Synchrotron Optics, edited by Tetsuya Ishikawa, Albert T. Macrander, James L. Wood, Proceedings of SPIE Vol. 5195 (SPIE, Bellingham, WA, 2003) · 0277-786X/03/$15 · doi: 10.1117/12.504098

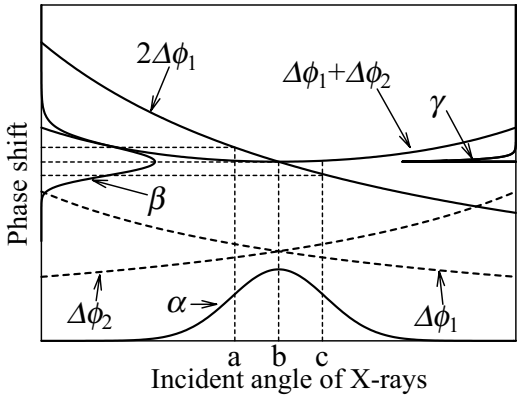

Figure 1. Phase shifts given by phase retarders as functions of incident angle of x rays. Phase shifts, $\Delta\phi_1$ and $\Delta\phi_2$ given by the first and second phase retarders arranged in a two-quadrant geometry, are drawn by dashed curves. Phase shifts given by the double phase retarders (solid curves) arranged in one-quadrant and two-quadrant geometries are given by $2\Delta\phi_1$ and by $\Delta\phi_1 + \Delta\phi_2$, respectively. This figure was reproduced from a separate paper.[19]

condition is sufficiently large compared with Darwin width, $\Delta\phi$ is approximately given by

$$\Delta\phi = \frac{c\,t}{\Delta\theta}. \tag{1}$$

Here, $\Delta\phi$ is phase shift between σ and π polarized components of the x rays transmitted by the phase retarder. t is thickness of the phase retarder crystal. c is a proportional constant which depends on wavelength of x rays and geometrical parameters of the phase retarder. Therefore, phase-shift inhomogeneity arises from angular divergence of the x rays incident on the phase retarder. The circumstances are clarified in Fig. 1. A curve $2\Delta\phi_1$ shows a phase-shift dependence on the incident angle of x rays when $t = t_0$, where t_0 is a thickness of the phase retarder. When the x rays have intensity distribution as α drawn on the abscissa of Fig. 1, the distribution α is projected on the curve $2\Delta\phi_1$ resulting in a phase-shift distribution as β drawn on the left ordinate of Fig. 1. However, if dashed phase-shift curves as $\Delta\phi_1$ and $\Delta\phi_2$ with two crystals of the same thickness $t_0/2$ can be made, phase-shift between σ and π polarized x rays consecutively transmitted by the two crystals will have a phase-shift curve as $\Delta\phi_1 + \Delta\phi_2$. The x-ray intensity distribution as α is projected on the curve $\Delta\phi_1 + \Delta\phi_2$ resulting in phase-shift distribution as γ drawn on the right ordinate of Fig. 1. γ is clearly suppressed compared with β. The condition described above can be realized using an x-ray optical system as shown in Fig. 2.

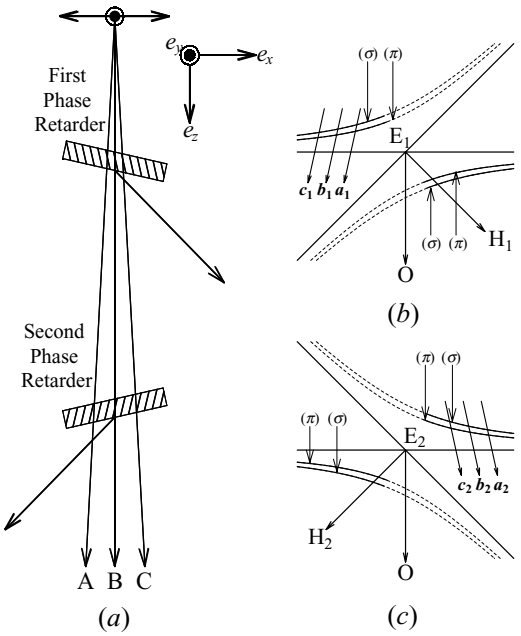

Figure 2. The left drawing (a) shows the practical arrangement of x-ray double phase retarder system compensating for the off-axis aberration of transmission-type phase retarder. The right upper (b) and right lower (c) drawings show dispersion surfaces in the reciprocal space corresponding to the first and second phase retarders, respectively. $\boldsymbol{a_1}$, $\boldsymbol{b_1}$ and $\boldsymbol{c_1}$ in (b) and $\boldsymbol{a_2}$, $\boldsymbol{b_2}$ and $\boldsymbol{c_2}$ in (c) are vectors normal to crystal surfaces of the first and second phase retarders which excite tie points on the dispersion surfaces with x-ray paths A, B and C, respectively, in the drawing (a).[19]

2.2. Estimation of the effect of compensation for off-axis aberration

Figure 3 shows experimental arrangements to estimate the effect of compensation for off-axis aberration. The experiment was performed at BL-15B$_1$ of the Photon Factory, Institute of Materials Structure Science. Two diamond (1 0 0)-oriented phase-retarder crystals were placed between monochromating polarizer and analyzer silicon crystals adjusted in a parallel nicol geometry within 0.1°. The polarizer and the analyzer gave four-bounced 5 1 1 reflection and were equipped with Hart-Rodrigues' offset mechanism. The offsets were applied to both the polarizer and analyzer crystals so that σ-π reflectivity ratios of the both crystals were calculated to be 3×10^9 at the nickel K-absorption edge (8333 eV). The Bragg angle of silicon 5 1 1 reflection was 45.38° at the energy of 8333 eV. The diamond phase-retarder crystals with diameters of about 5 mm, whose thickness were 313μm (PR$_1$) and 314μm (PR$_2$), were mounted on

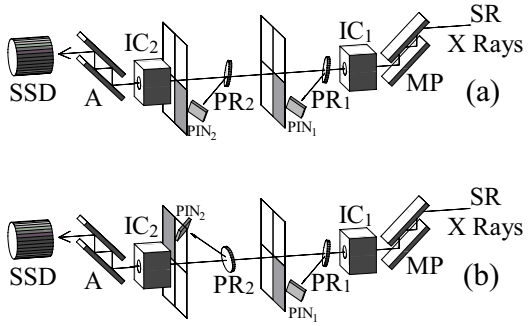

Figure 3. Experimental arrangements for estimating the effect of the compensation for off-axis aberration. MP : silicon 5 1 1 monochromating polarizer, PR_1 and PR_2 : first and second diamond 1 1 1 phase retarders, IC_1 : ionization chamber monitoring the x -rays Bragg-reflected by the monochromating polarizer, PIN_1 and PIN_2 : PIN photodiodes monitoring the x rays Bragg-reflected by the first and the second phase retarder, IC_2 : ionization chamber monitoring the x rays transmitted by the double phase retarders, A : silicon 5 1 1 analyzer crystal arranged in a parallel nicol geometry with the polarizer.[19]

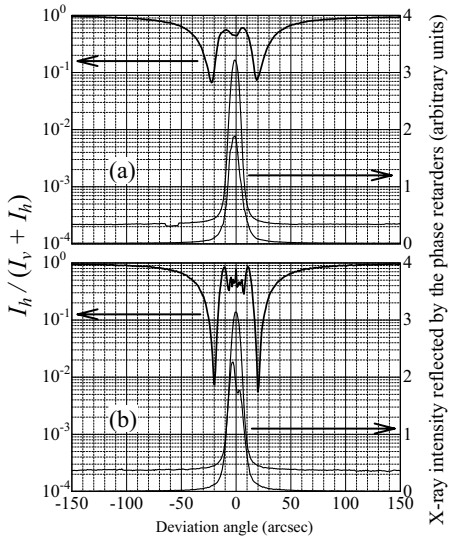

Figure 4. Rate of residual horizontally polarized component of x rays which was converted from the horizontal polarization by the double phase retarder systems. (a) and (b) correspond to the geometries shown in Figs. 3(a) and 3(b).[19]

two goniometers whose axes are perpendicular to the transmission x-ray beam axis and inclined by 45° from the horizontal plane so that the diamond crystals gave 1 1 1 reflection in an asymmetric Laue geometry. About 47% of incident photons were transmitted by the two diamond crystals. The horizontally polarized component of the transmitted x rays was measured with a germanium solid state detector (SSD) for two-type double phase-retarder geometries shown in Figs. 3 (a) and 3 (b) rotating the two diamond crystals simultaneously from lower to higher angle side. (a) corresponds to a single phase retarder with a thickness of 627 μm (313μm + 314μm). (b) is a two-quadrant phase-retarder system.

Figures 4(a) and 4(b) are experimental results corresponding to the arrangements of Figs. 3(a) and 3(b). In both Figs. 4(a) and 4(b), dips are observed at ±20arcsec, which means that approximately vertically polarized x rays are generated. The depths of dips in Fig. 4(b) are more than one order of magnitude as deep as those in Fig. 4(a). Maximum degree of vertical polarization was calculated to be 0.99 from the depth of dips in Fig. 4(b), while it was 0.87 in the case of Fig. 4(a). Furthermore, fine oscillatory profiles are observed between the two dips in Fig. 4(b) whereas such oscillations are blurred and cannot be observed in Fig. 4(a). This results also verify the effect of compensation for off-axis aberration

3. FOUR-QUADRANT PHASE-RETARDER SYSTEM

3.1. Existence of chromatic aberration of the transmission-type phase retarder

Figure 5 shows dispersion surfaces with wavelengths of x rays, λ and $\lambda+\Delta\lambda$, where $\Delta\lambda$ is a small positive differential value of wavelength. According to the x-ray dynamical diffraction theory, the amplitude of transmitted x rays is mainly occupied by the amplitude excited with tie points $P_1^{(\sigma)}$ and $P_1^{(\pi)}$ on the upper branches of dispersion surfaces when x rays are incident on the phase-retarder crystal with an angle lower than the Bragg angle. To the contrary, when x rays are incident with a higher angle, tie points on the lower branches play an important role with respect to the transmitted x rays. These circumstances are shown in Fig. 5 with important and less important parts of dispersion surfaces drawn by solid and dashed curves, respectively. In Fig. 5, the phase shift is considered to be proportional to σ-π gap of dispersion surfaces drawn by solid curves *e.g.* distance between $P_1^{(\sigma)}$ and $P_1^{(\pi)}$ in Fig. 5. On the other hand, since $\Delta\lambda$ is assumed to be a small value, dispersion surfaces around the Lorentz point L_2 are considered to be the same as those around the Lorentz point L_1 without change in σ-π dispersion-surface gap. Here, let us introduce a phase-shift value $\Delta\phi^{(\sigma-\pi)}$ defined by

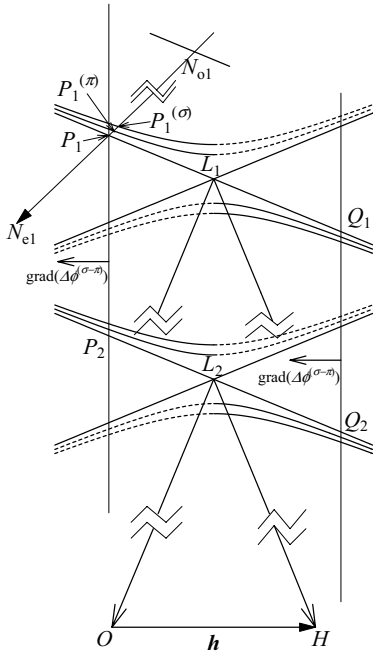

Figure 5. Two sets of dispersion surfaces corresponding to wavelengths λ (upper) and $\lambda + \Delta\lambda$ (lower). When x rays with a wavelength of λ whose wave number vector of $\overrightarrow{N_{o1}O}$ are incident on a phase-retarder crystal, a vector $\overrightarrow{N_{o1}N_{e1}}$ normal to the surfaces of the crystal stimulates tie points $P_1^{(\sigma)}$ and $P_1^{(\pi)}$ on the dispersion surfaces, resulting in phase-shift value $\Delta\phi^{(\sigma-\pi)}$ due to dispersion-surface gap $P_1^{(\sigma)}P_1^{(\pi)}$. This figure was reproduced from a separate paper.[20]

$\Delta\phi^{(\sigma-\pi)} = \phi^{(\sigma)} - \phi^{(\pi)}$, where $\phi^{(\sigma)}$ and $\phi^{(\pi)}$ are phase-shift advances of σ- and π-polarized x rays transmitted by the phase retarder compared with x rays transmitted by an atmospheric path. Real value $\Delta\phi^{(\sigma-\pi)}$ is distributed as a function in the three-dimensional reciprocal space in which Fig. 5 is drawn. For example, when tie points $P_1^{(\sigma)}$ and $P_1^{(\pi)}$ are excited with a crystal-surface normal $\overrightarrow{N_{o1}N_{e1}}$, the value of $\Delta\phi^{(\sigma-\pi)}$ at point P_1 in Fig. 5 is given by

$$\Delta\phi^{(\sigma-\pi)}(P_1) \simeq -2\pi\ \overrightarrow{P_1^{(\sigma)}P_1^{(\pi)}} \cdot \frac{\overrightarrow{N_{o1}N_{e1}}}{\left|\overrightarrow{N_{o1}N_{e1}}\right|}\ t. \qquad (2)$$

Here, t is the thickness of the phase-retarder crystal. Even if λ is changed to $\lambda + \Delta\lambda$, $\Delta\phi^{(\sigma-\pi)}$ at point P_2 is given by

$$\Delta\phi^{(\sigma-\pi)}(P_2) = \Delta\phi^{(\sigma-\pi)}(P_1). \qquad (3)$$

Therefore, line P_1P_2 is a locus of point P, where

$$\Delta\phi^{(\sigma-\pi)}(P) = \Delta\phi^{(\sigma-\pi)}(P_1). \qquad (4)$$

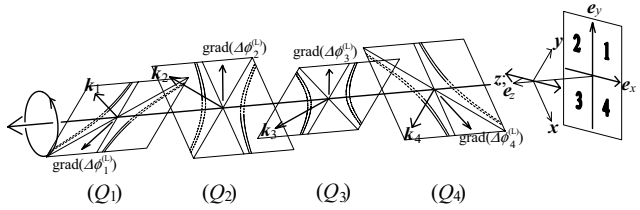

Figure 6. Principle of compensation for both off-axis and chromatic aberrations of transmission-type x-ray phase retarder by using four-quadrant phase retarder system. In parts (Q_1), (Q_2), (Q_3) and (Q_4), dispersion surfaces corresponding to phase retarders giving Bragg reflections in the directions of the first, second, third and fourth quadrants, respectively, viewed from the downstream direction, are drawn.[20]

With a similar consideration, line Q_1Q_2 is a locus of point Q, where

$$\Delta\phi^{(\sigma-\pi)}(Q) = \Delta\phi^{(\sigma-\pi)}(Q_1). \qquad (5)$$

Here, gradient of phase shift grad($\Delta\phi^{(\sigma-\pi)}$) is a vector perpendicular to contours P_1P_2 and Q_1Q_2. Now let us consider the direction of grad($\Delta\phi^{(\sigma-\pi)}$). In the vicinity of point P_1, the sign of $\Delta\phi^{(\sigma-\pi)}$ is negative and $\left|\Delta\phi^{(\sigma-\pi)}\right|$ decreases with P_1 being further from the Lorentz point L_1. Therefore, grad($\Delta\phi^{(\sigma-\pi)}$) is directed to the left. On the other hand, in the vicinity of point Q_1, $\Delta\phi^{(\sigma-\pi)}$ is positive and $\left|\Delta\phi^{(\sigma-\pi)}\right|$ decreases with Q_1 being further from L_1. Therefore, also in this case, grad($\Delta\phi^{(\sigma-\pi)}$) is directed to the left. Then, grad($\Delta\phi^{(\sigma-\pi)}$) is always directed to the left. Since, as shown in Fig. 5, grad($\Delta\phi^{(\sigma-\pi)}$) has components both parallel and perpendicular to the direction of x-ray transmission, the transmission-type phase retarder suffers from not only off-axis aberration but also chromatic aberration.

3.2. Principle of compensation for both off-axis and chromatic aberrations

Figure 6 shows four planes on which dispersion surfaces are drawn together with wavevector $\mathbf{k}_n$ ($n \in \{1, 2, 3, 4\}$) of x rays reflected by four phase-retarder crystals. In the right part of Fig. 6, x-y-z and e_x-e_y-e_z orthogonal coordinate systems are drawn. $\mathbf{z}(= \mathbf{e}_z)$ is a unit vector in the direction of transmitted x-ray propagation. $\mathbf{e}_x$ and $\mathbf{e}_y$ are horizontal and vertical unit vectors, respectively. $\mathbf{x}$ and $\mathbf{y}$ are unit vectors which are rotated from $\mathbf{e}_x$ and $\mathbf{e}_y$ around $\mathbf{z}(= \mathbf{e}_z)$ by $-45°$. The incident monochromatized synchrotron x rays are linearly polarized in the direction of $\mathbf{e}_x$. Here, let us define the

polarity of elliptical polarization. When the locus of end point of electric displacement vector is left-screwed if the time is stopped, the electric displacement vector rotates counterclockwise vied from downstream direction with the progress of time. In this situation, the phase of y-polarized component of x rays has to be retarded against x-polarized component. Therefore, for transforming the incident horizontal polarization into a left-screwed elliptical polarization with a small ellipticity, the phase retarders have to work so as to give a slight phase retardation to y-polarized component of x rays against x-polarized component. In the cases of the first- and third-quadrant phase retarders giving the Bragg reflection whose dispersion surfaces are drawn in parts (Q_1) and (Q_3) in Fig. 6, y polarization is π polarization. To the contrary, in the cases of second- and fourth-quadrant phase retarders whose dispersion surfaces are drawn in parts (Q_2) and (Q_4) in Fig. 6, y polarization is σ polarization. Here, let us define a small phase shift $\Delta\phi_n^{(L)}$ which translates horizontal polarization to left-screwed elliptical polarization with the nth $(n \in \{1,2,3,4\})$ quadrant phase retarder as follows,

$$\Delta\phi_n^{(L)} = \phi_n^{(\sigma)} - \phi_n^{(\pi)} = \Delta\phi_n^{(\sigma-\pi)}, \quad \text{where } n \in \{1,3\}, \tag{6}$$

$$\Delta\phi_n^{(L)} = \phi_n^{(\pi)} - \phi_n^{(\sigma)} = -\Delta\phi_n^{(\sigma-\pi)}, \quad \text{where } n \in \{2,4\}. \tag{7}$$

Therefore,

$$\mathrm{grad}(\Delta\phi_n^{(L)}) = \mathrm{grad}(\Delta\phi_n^{(\sigma-\pi)}), \quad \text{where } n \in \{1,3\}, \tag{8}$$

$$\mathrm{grad}(\Delta\phi_n^{(L)}) = -\mathrm{grad}(\Delta\phi_n^{(\sigma-\pi)}), \quad \text{where } n \in \{2,4\}. \tag{9}$$

This reversal of sign between (8) and (9) is very important to compensate for chromatic aberration. This situation is more clarified in Fig. 7. Figure 7 shows dispersion surfaces together with $\mathrm{grad}(\Delta\phi_n^{(L)})$. Left-hand and right-hand drawings of Fig. 7 show the cases of $n \in \{1,3\}$ and $n \in \{2,4\}$, respectively. As x-y-z coordinate system is drawn in upper part of Fig. 7, the plane of right-hand drawing is rotated by $-90°$ with respect to the plane of left-hand drawing of Fig. 7. $\mathrm{grad}(\Delta\phi_1^{(L)}) + \mathrm{grad}(\Delta\phi_3^{(L)})$ is directed to downstream of transmitted x rays while $\mathrm{grad}(\Delta\phi_2^{(L)}) + \mathrm{grad}(\Delta\phi_4^{(L)})$ is directed to upstream to the contrary. Therefore, by controlling four phase retarders so that $\mathrm{grad}(\Delta\phi_n^{(L)})$ $(n \in \{1,2,3,4\})$ have the identical value, the condition $\sum_4^{n=1} \mathrm{grad}(\Delta\phi_n^{(L)}) = 0$ can be realized and both the off-axis and chromatic aberrations are compensated with the four-quadrant phase retarder system.

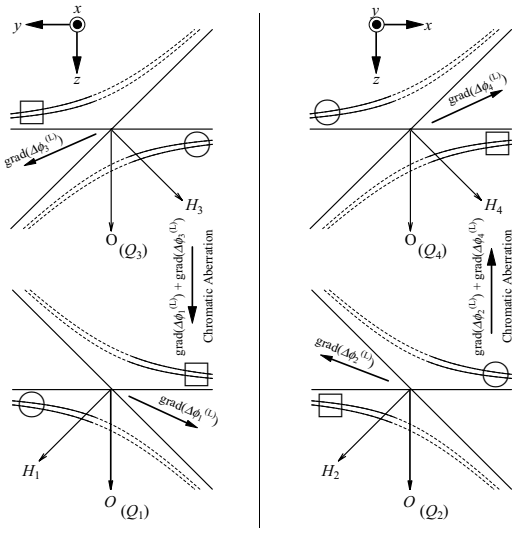

Figure 7. Four dispersion surfaces of the four-quadrant phase-retarder system. These figures clarifies three-dimensional Fig. 6 by drawing dispersion surfaces of odd-number-th-quadrant phase retarders in left part and those of even-number-th-quadrant phase retarders in right part. Suffix n $(n \in \{1,2,3,4\})$ in Q_n, H_n and $\Delta\phi_n^{(L)}$ corresponds to n-th-quadrant phase retarder. The planes of drawings are rotated by 90° around the direction of vector **z** (direction of transmitted x-ray propagation) between left- and right-hand drawings. It can be understood that directions of chromatic aberrations due to odd-number-th-quadrant and even-number-th-quadrant phase retarders are contrary and then cancelled out with each other. A left-screwed polarization $(\pi > \sum_{n=1}^{4} \phi_n^{(L)}) > 0)$ is generated by using angular regions indicated by four circles. On the other hand, a right-screwed polarization $(0 > \sum_{n=1}^{4} \phi_n^{(L)}) > -\pi)$ is generated at regions indicated by four squares.[20]

3.3. Estimation of the effect of compensation for aberrations

Figure 8 shows experimental arrangements to estimate the effect of compensation for the aberrations. Four phase-retarder (1 0 0)-oriented diamond crystals PR_n $(n \in \{1,2,3,4\})$ with thickness of 318μm, 314μm, 301μm and 313μm were placed between polarizer and analyzer crystals. PR_n $(n \in \{1,2,3,4\})$ were set so as to give 1 1 1 reflection in asymmetric Laue geometries. The polarizer MP worked also as a monochromator and then water-cooled. The polarizer and analyzer were channel-cut silicon crystals giving four-bounced 4 2 2 reflection in a symmetric Bragg geometry and were equipped with Hart-Rodrigues' offset mechanism.[8]

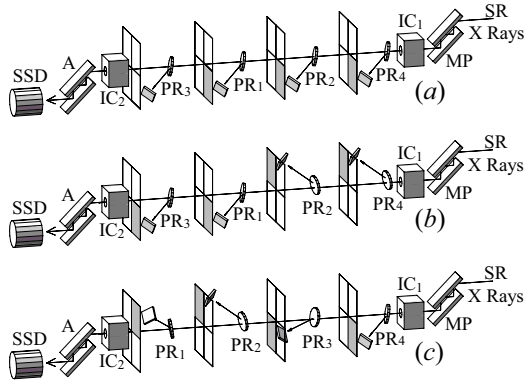

Figure 8. Experimental arrangements of quadruple phase retarders in (a) one-quadrant, (b) two-quadrant and (c) four-quadrant geometries. MP: a silicon channel-cut monochromating polarizer equipped with Hart-Rodrigues' offset mechanism[8] giving four-bounced 422 reflection in a symmetric Bragg geometry, A: an analyzer crystal similar to the polarizer, PR_1, PR_2, PR_3 and PR_4: diamond (100)-oriented phase retarder crystals giving 111 reflection in an asymmetric Laue geometry whose thickness are 318 μm, 314 μm, 301 μm and 313 μm, respectively, IC_1 and IC_2: ionization chambers, SSD: a solid state detector of germanium. Bragg-reflected x rays from four phase retarders are monitored by four PIN photo-diodes.[20]

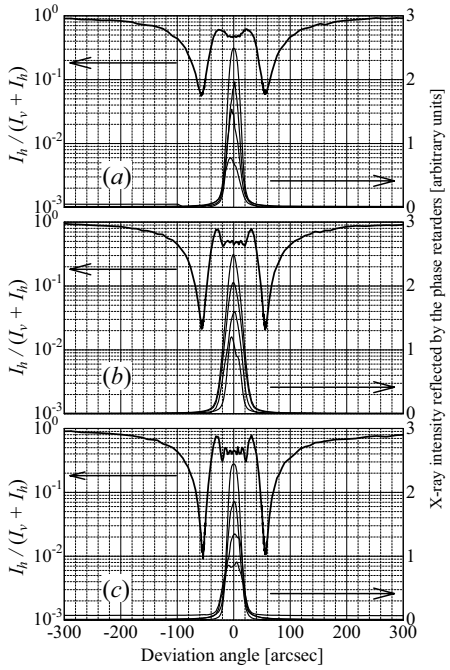

Figure 9. Rate of residual horizontally polarized component of x rays whose polarization state was converted from the horizontal polarization by quadruple phase retarder systems. The abscissa is $\Delta\theta_4$. (a), (b) and (c) correspond to the geometries shown in Figs. 8(a), 8(b) and 8(c).[20]

The energy of x rays was adjusted to be 7709 eV (cobalt K-absorption edge). Throughput of x rays transmitted by the four phase retarders was 0.13. The Bragg angle of silicon 4 2 2 reflection was 46.50°. σ-π reflectivity ratio of polarizer and analyzer was calculated to be $> 10^7$ based on the dynamical theory. In the case of Figs. 8(a) and 8(b), horizontally polarized component of x rays were measured with SSD behind the analyzer rotating the four phase retarders from lower to higher angle side of the Bragg condition simultaneously keeping the following condition:

$$\frac{t_1}{{\Delta\theta_1}^2} = \frac{t_2}{{\Delta\theta_2}^2} = \frac{t_3}{{\Delta\theta_3}^2} = \frac{t_4}{{\Delta\theta_4}^2}. \qquad (10)$$

where t_n and $\Delta\theta_n$ are thickness and deviation angle from the Bragg condition of PR_n ($n \in \{1,2,3,4\}$). (10) is a condition that differentiation of (1) by $\Delta\theta$ is the same value for PR_n ($n \in \{1,2,3,4\}$) resulting in the identical value of $\left|\mathrm{grad}(\Delta\phi_n^{(L)})\right|$. In the case of Fig. 8(c), PR_2 and PR_4 were rotated from lower to higher angle side while PR_1 and PR_3 were rotated from higher to lower angle side keeping the condition of (10). This is owing to the sign reversal between (6) and (7).

Figs. 9(a), 9(b) and 9(c) show experimental results corresponding to experimental arrangements Figs. 8(a), 8(b) and 8(c) performed at BL-4A of the Photon Factory. Two dips are observed at $\Delta\theta_4 \simeq \pm 60$ arcsec in Figs. 9(a), 9(b) and 9(c). This indicates that maximum degrees of vertically linear polarization were created there. The maximum degree of vertical polarization 0.98 was obtained in the case of Fig. 9(c) with a condition that horizontal beam divergence and energy spread of incident x rays were 45 arcsec and 1.5 eV, respectively.[20] In the cases of Figs. 9(a) and 9(b), the maximum degrees of vertical polarization were 0.89 and 0.96, respectively.[20] It is clear that the two-quadrant geometry corresponding to the two-quadrant phase retarder system[19] creates higher degrees of vertical polarization than the one-quadrant geometry corresponding to a single phase retarder. This is owing to the effect of compensation for off-axis aberration. In addition, the four-quadrant geometry gives higher degrees of vertically linear polarization than the two-quadrant geometry. This means that not only the off-axis aberration but also the chromatic aberration are compensated with the four-quadrant geometry. It is noteworthy that fine oscillatory profiles which reveal rapid changes of phase shift are found between the dips in the vicinity

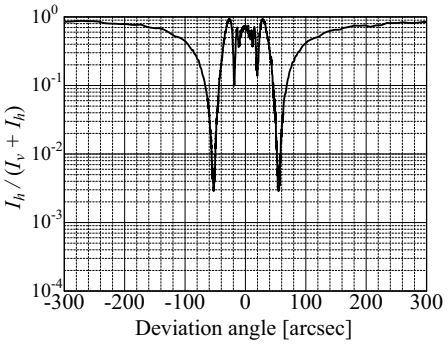

Figure 10. Rate of residual horizontally polarized component of x rays which was converted from the horizontal polarization by the four-quadrant phase retarder system.[20] This was measured at station BL-15C of the Photon Factory whose distance from radiation source is about 30m. The angular divergence and energy spread of incident x rays were 20 arcsec and 0.5 eV, respectively, The abscissa is $\Delta\theta_4$.

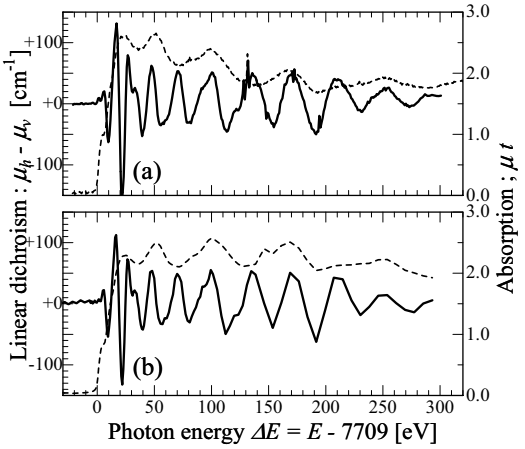

Figure 11. X-ray natural linear dichroism (XNLD) (a) measured from a rotation angle of polarization using an x-ray polarimeter[27] and (b) measured with linear polarization switching technique using the four-quadrant phase retarder system.[20] The sample was a $11\overline{2}0$-oriented *hcp* cobalt single crystal foil with a thickness of 11μm.

of the Bragg condition, in the cases of (b) and (c). Such oscillatory profiles are blurred and not found due to the aberrations in the case of (a). The oscillatory profiles can be more clearly observed in the case of (c) than in the case of (b), resulting from the effect of compensation for the chromatic aberration.

Figure 10 shows result of an experiment whose arrangement was Fig. 8(c) performed at BL-15C of the Photon Factory with a condition that horizontal beam divergence and energy spread of incident x rays were 25 arcsec and 0.5 eV, respectively. The maximum degree of vertical polarization was 0.994.

4. ADVANTAGE OF THE ABERRATION-COMPENSATING PHASE-RETARDER SYSTEMS IN HIGH ENERGY REGION

In higher energy region, Fourier coefficient of electric susceptibility of the phase retarder crystal decreases and the phase retarder has to work with deviation angle, $\Delta\theta$ closer to the Bragg condition where grad($\Delta\theta$) has greater values, and absorption coefficient decreases. Therefore, the phase retarder has to be thicker in the high energy region. In the case of a single phase retarder, the maximum energy where it generates sufficiently high degree of polarization, is limited by the thickness of diamond crystal available. In the case of the four-quadrant phase-retarder system, the limitation of effective thickness of diamond becomes 4 times as great as the case of a single phase retarder. Therefore, the four-quadrant phase-retarder system has a great advantage together with the effect of compensation for aberrations, particularly in the high energy region.

5. APPLICATIONS OF THE ABERRATION-COMPENSATING PHASE-RETARDER SYSTEMS

We have successfully measured x-ray natural circular dichroism (XNCD)[21] by using the two-quadrant and four-quadrant phase-retarder systems. Furthermore, x-ray natural linear dichroism (XNLD) imaging,[22] x-ray magnetic circular dichroism (XMCD) imaging[23,24] and x-ray magnetic linear dichroism (XMLD) imaging[24–26] have been performed for the first time by using the two-quadrant phase-retarder-system. Particularly, XMLD measurement was the first measurement in hard x-ray region. Two-quadrant or four-quadrant phase retarder system is chosen depending on the throughput and the degree of polarization required for the measurement.

Figure 11 shows XNLD spectra of $11\overline{2}0$-oriented *hcp* cobalt single crystal foil (11μm thick) measured by two methods (see figure caption). The precision of XNLD spectrum measured with linear polarization switching (Fig. 11(b)) is as high as that measured with an x-ray polarimeter[27] (Fig. 11(a)).

6. SUMMARY

Two-quadrant and four-quadrant phase retarder systems which can compensate aberrations of the

transmission-type phase retarder have been developed. They can generate higher degree of polarization than a single phase retarder and have been successfully applied to measurements of various x-ray polarization phenomena. They have a great advantage particularly in higher energy region over a single phase retarder, and are expected to expand the energy range in which polarization-controlled x rays can be utilized.

ACKNOWLEDGMENTS

The present work was performed under the approval of Photon Factory Program Advisory Committee (Proposal No. 97G-179, 97G-180, 99S2-003), and is one of the activities of Active Nano-Characterization and Technology Project financially supported by Special Coordination Funds of the Ministry of Education, Culture, Sports, Science and Technology of the Japan Government. The authors are indebted to Dr. K. Sato of National Institute of Advanced Industrial Science and Technology for his co-working and technical assistance. The adjustment of diamond phase retarders was performed at High-Power X-Ray Laboratory, Institute of Engineering Innovation, School of Engineering, The University of Tokyo.

REFERENCES

1. G. Moliere *Ann. Phys.* **35**, p. 297, 1939.
2. P. Skalicky and C. Malgrange *Acta Crystallogr. Sec. A* **28**, pp. 501–507, 1972.
3. M. Hart *Philos. Mag. B* **38**, pp. 41–56, 1978.
4. S. Annaka, T. Suzuki, and K. Onoue *Acta Crystallogr. Sec. A* **36**, pp. 151–152, 1980.
5. S. Annaka *J. Phys. Soc. Jpn.* **51**, pp. 1927–1931, 1982.
6. J. A. Golovchenko, B. M. Kincaid, R. A. Lvesque, A. E. Meixner, and D. R. Kaplan *Phys. Rev. Lett.* **57**, pp. 202–205, 1986.
7. D. M. Mills *Phys. Rev. B* **36**, pp. 6178–6181, 1987.
8. M. Hart and A. R. D. Rodrigues *Philos. Mag. B* **40**, pp. 149–157, 1979.
9. K. Hirano, K. Izumi, T. Ishikawa, S. Annaka, and S. Kikuta *Jpn. J. Appl. Phys.* **30**, pp. L407–L410, 1991.
10. T. Ishikawa, K. Hirano, and S. Kikuta *J. Appl. Crystallogr.* **24**, pp. 982–986, 1991.
11. K. Hirano, T. Ishikawa, S. Koreeda, K. Fuchigami, K. Kanzaki, and S. Kikuta *Jpn. J. Appl. Phys.* **31**, pp. L1209–L1211, 1992.
12. T. Ishikawa, K. Hirano, K. Kanzaki, and S. Kikuta *Rev. Sci. Instrum.* **63**, pp. 1098–1103, 1992.
13. K. Hirano, T. Ishikawa, and S. Kikuta *Nucl. Instrum. Methods Phys. Res. A* **336**, pp. 343–353, 1993.
14. K. Hirano, T. Ishikawa, and S. Kikuta *Rev. Sci. Instrum.* **66**, pp. 1604–1609, 1995.
15. K. Hirano *J. Cryst. Soc. Jpn.* **38**, pp. 221–228, 1996. [in japanese].
16. C. Giles, C. Malgrange, J. Goulon, F. Bergevin, C. Vettier, E. Dartyge, A. Fontaine, C. Giorgetti, and S. Pizzini *J. Appl. Crystallogr.* **27**, pp. 232–240, 1994.
17. K. Hirano and H. Maruyama *Jpn. J. Appl. Phys.* **36**, pp. L1272–L1274, 1997.
18. M. Suzuki, N. Kawamura, M. Mizumaki, A. Urata, H. Maruyama, S. Goto, and T. Ishikawa *Jpn. J. Appl. Phys.* **37**, pp. L1488–L1490, 1998.
19. K. Okitsu, Y. Ueji, K. Sato, and Y. Amemiya *J. Synchrotron Rad.* **8**, pp. 33–37, 2001.
20. K. Okitsu, Y. Ueji, K. Sato, and Y. Amemiya *Acta Crystallogr. Sec. A* **58**, pp. 146–154, 2002.
21. Y. Ueji, K. Okitsu, K. Sato, and Y. Amemiya *J. Jpn. Soc. Synchrotron Rad. Res.* **13**(1), pp. 48–56, 2000. [in japanese].
22. K. Sato, K. Okitsu, Y. Ueji, T. Matsushita, and Y. Amemiya *J. Synchrotron Rad.* **7**, pp. 368–373, 2000.
23. K. Sato, Y. Ueji, K. Okitsu, T. Matsushita, and Y. Amemiya *J. Synchrotron Rad.* **8**, pp. 1021–1026, 2001.
24. K. Sato, Y. Ueji, K. Okitsu, T. Matsushita, J. Saito, T. Takayama, and Y. Amemiya *J. Magn. Soc. Jpn.* **25**, p. 206, 2001.
25. K. Sato, Y. Ueji, K. Okitsu, T. Matsushita, J. Saito, T. Takayama, and Y. Amemiya *J. Magn. Soc. Jpn.* **26**, p. 238, 2002.
26. K. Sato, Y. Ueji, K. Okitsu, T. Matsushita, J. Saito, T. Takayama, and Y. Amemiya *Phys. Rev. B* **65**, pp. 134408 1–6, 2002.
27. K. Okitsu, T. Oguchi, H. Maruyama, and Y. Amemiya *J. Synchrotron Rad.* **5**, pp. 995–997, 1998.